The Autonomic Nervous System Can Compensate for Hypocalcemia-Induced Bradycardia in Human and Rabbit Sinoatrial Node Cell Models

Moritz Linder[1], Tomas Stary[1], Gergő Bitay[2], Norbert Nagy[2], Axel Loewe[1]

[1] Institute of Biomedical Engineering, Karlsruhe Institute of Technology (KIT), Karlsruhe, Germany
[2] Department of Pharmacology and Pharmacotherapy, Albert Szent-Györgyi Medical School, University of Szeged; Szeged, Hungary

Abstract

Every regular heartbeat is initiated by cyclic spontaneous depolarisations of sinoatrial node cells (SANCs). Altered electrolyte levels, typically occurring in chronic kidney disease (CKD) patients, and the autonomic nervous system (ANS) highly influence pacemaking of the heart. Thus, the effects of sympathetic stimulation and hypocalcemia on the beating rate (BR) were assessed. Therefore, we integrated the β-adrenergic (β-AR) signalling cascade of Behar et al., into the Severi et al. (rabbit) and Fabbri et al. (human) SANC models. To mimic conditions in patients suffering from CKD, extracellular Ca^{2+} ($[Ca^{2+}]_o$) (0.6 to 1.8 mM) and isoprenaline concentrations ([ISO]) (0.0 to 1000.0 nM) were varied. The extended models predicted that for decreased $[Ca^{2+}]_o$, an exponential-like increase of [ISO] restored the basal BR. In particular, for 1.2 mM $[Ca^{2+}]_o$, 15.5 and 7.3 nM [ISO] for the Severi and Fabbri model restored the initial conditions. With $[Ca^{2+}]_o$ further reduced to 0.6 mM, 60.0 and 41.7 nM [ISO] were required. A sudden loss of sympathetic tone resulted in extreme bradycardia or stopped automaticity. The results suggest that hypocalcemic bradycardia can be compensated by an increased sympathetic tone. The integration of the β-AR pathways led to an exponential-like increase of the BR. This combined model may help understanding the pathomechanisms of sudden cardiac death in CKD.

1. Introduction

Initiated through regular excitations generated in the sinus node, the natural pacemaker function in mammals is governed by the intricate interaction of the Ca^{2+} and membrane clock, the so-called coupled clock mechanism. This comprises tight control over the sensitive balance of inward and outward transmembrane currents during the diastolic depolarisation (DD) phase and the complex interplay of both mechanisms during the action potential (AP). Several factors, such as the extracellular milieu and the autonomic nervous system (ANS) regulate the electrophysiology and, thus, the beating rate (BR) [1]. However, the effects of β-AR stimulation on critical membrane and sarcoplasmic reticulum (SR) currents are barely represented as continuous variables in current computational models of sinoatrial node cells (SANCs).

Numerical modelling of SANCs and the influencing components could shed light on the underlying pathomechanisms of serious diseases and help to overcome the lack of experimental data. Patients suffering from chronic kidney disease (CKD) have a 14-fold increased risk of dying from sudden cardiac death (SCD) [2], which might be related to changes in electrolyte concentrations, especially hypocalcemia, caused by haemodialysis (HD) or renal failure [3]. Furthermore, Ishii et al. documented elevated plasma catecholamines and enhanced sensitivity to norepinephrine [4], while Converse et al. found increased muscular sympathetic nerve activity in patients with end-stage renal disease [5]. Consequently, it is hypothesised that an increased sympathetic tone can compensate hypocalcemia-induced bradycardia to a certain extent, whereas a sudden loss under hypocalcemic conditions could lead to severe bradycardia and SCD in CKD patients.

In this study, the effects of altered extracellular Ca^{2+} ($[Ca^{2+}]_o$) and isoprenaline concentrations ([ISO]) were investigated in an extended computational rabbit and human SANC model by Severi et al. [6] and Fabbri et al. [7], respectively.

2. Methods

The intention of this *in silico* study was to analyse the concentration-dependent compensatory effect of [ISO] in reference to decreasing $[Ca^{2+}]_o$ in the SANC models of Severi et al. (rabbit) [6] and Fabbri et al. (human) [7] as provided in the CellML [8] repository. These models enable to simulate single cells either in basal conditions or under the influence of 1000.0 nM [ISO]. However, to ensure graded changes of the sympathetic tone, the beta-adrenergic (β-AR) signalling cascade based

on the work of Behar et al. [9] was adjusted and integrated into these models. This included chages in the cyclic adenosinemonophosphate (cAMP)-protein kinase A (PKA) relationship, which led to a slightly different basal PKA activity level as well as the continuous modulation of I_{CaL}, I_f, I_{NaK}, I_{Ks}, phospholamban (PLB) regulating the sarcoplasmic/endoplasmic reticulum Ca^{2+}-adenosintriphosphatase (SERCA) and the ryanodine receptor (RyR). Only I_f was directly affected by cAMP binding to the channel, whereas the PKA-dependent phosphorylation modulated all the other targets.

Furthermore, different Ca^{2+}-related association and dissociation constants (kb_{CM} & kf_{CM}) in the original and extended models, along with differences in the fractional occupancy of calmodulin by Ca^{2+} in the myoplasm (fCMi), required enhancements in the calculation of the cAMP concentration. Therefore, the constant defining the maximal adenylyl cyclase (AC) activation by Ca^{2+} (K_{Ca}) was altered in both models and a pre-factor (K_{fab} = 4.646336) was added in case of the Fabbri model.

The models were solved using openCARP [10] with Rush-Larsen and forward Euler integration schemes. Simulation time was set to 1000 s with the last 100 s taken into consideration. This ensured transient oscillations to equilibrate, which resulted in a stable limit cycle length. The simulations covered $[Ca^{2+}]_o$ from 0.6 to 1.8 mM with a step size of 0.2 mM. To provide insight into the expected non-linear behaviour of the models in reference to varying [ISO], the simulated concentrations ranged from 0.0 to 10.0 nM in steps of 2.5 nM, from 10.0 to 100.0 nM in steps of 25.0 nM and 100.0 to 1000.0 nM in steps of 250.0 nM.

3. Results

In the basal state without sympathetic stimulation, automaticity of the extended Severi model stopped at 1.3 mM $[Ca^{2+}]_o$ and at 1.2 mM in case of the extended Fabbri model. Analyzing the specific contributions, the main pacemaker current in the extended Severi model is I_f, whereas I_{CaL} plays a more important role in the extended Fabbri model. Thus, the BR in the extended Fabbri model was more sensitive to hypocalcemia.

A detailed analysis of the β-AR effect on the SANC models is provided in Fig. 1, which shows selected currents of the extended Severi and Fabbri model for a complete AP cycle in the ground state and under the influence of 10.0 nM [ISO]. During the AP upstroke, the β-AR stimulation led to an increase in I_{Ks} and I_{NaK}, which attenuated the influence of I_{Kr}. The large effects on I_{CaL} during the DD decreased the impact of I_f, I_{NaCa} and I_{CaT}.

The influence of graded changes in $[Ca^{2+}]_o$ and [ISO] are shown in Fig. 2. While the influence of $[Ca^{2+}]_o$ appeared to be rather linear for high [ISO], especially for the extended human SANC model, the BRs increased logarithm-like for smaller [ISO].

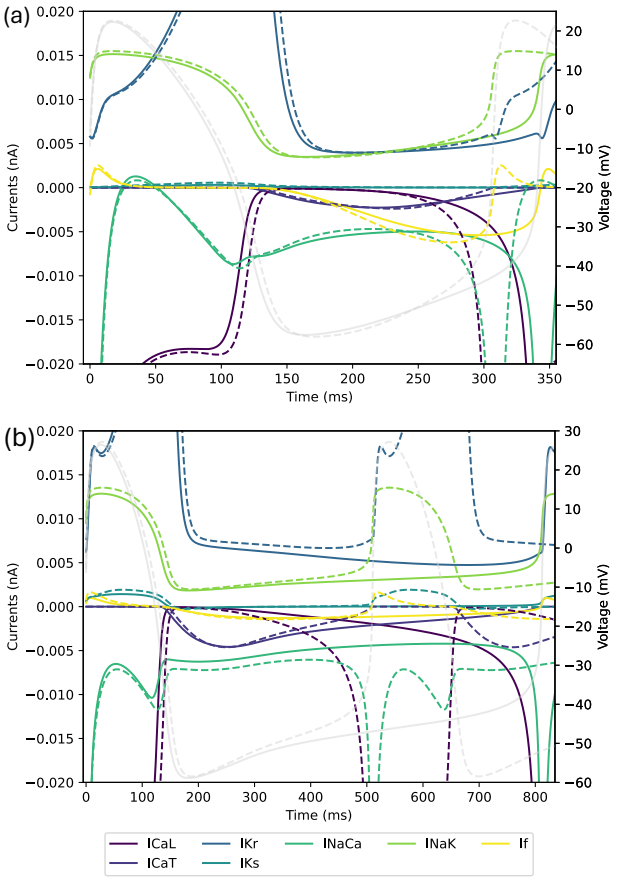

Figure 1: (a) selected currents of the extended Severi model during one AP cycle under basal conditions (solid) and after β-AR stimulation with 10.0 nM [ISO] (dashed). Transmembrane voltage in light grey (background). (b) results of the extended Fabbri model during one AP cycle under basal conditions (solid) and after β-AR stimulation with 10.0 nM [ISO] (dashed). Transmembrane voltage in light gray (background).

Analysing the compensatory effect of [ISO] in combination with hypocalcemia revealed that for linear decreases in $[Ca^{2+}]_o$ an exponential-like increase in [ISO] was needed to maintain the basal BR (Fig. 3). When simulating the extended Severi model with $[Ca^{2+}]_o$ of 1.2 mM, 15.5 nM [ISO] restored the initial BR, while for the extended Fabbri model, 7.3 nM were sufficient, indicating that the extended Fabbri model is not only more sensitive to changes in $[Ca^{2+}]_o$ but also to sympathetic stimulation. Further decreasing the $[Ca^{2+}]_o$ to a minimum of 0.6 mM required [ISO] of 60.0 nM and 41.7 nM, respectively. Mimicking a sudden loss of sympathetic tone at low $[Ca^{2+}]_o$ unmasked the low basal BR under hypocalcemic conditions. Considering the extended Severi model, this led to

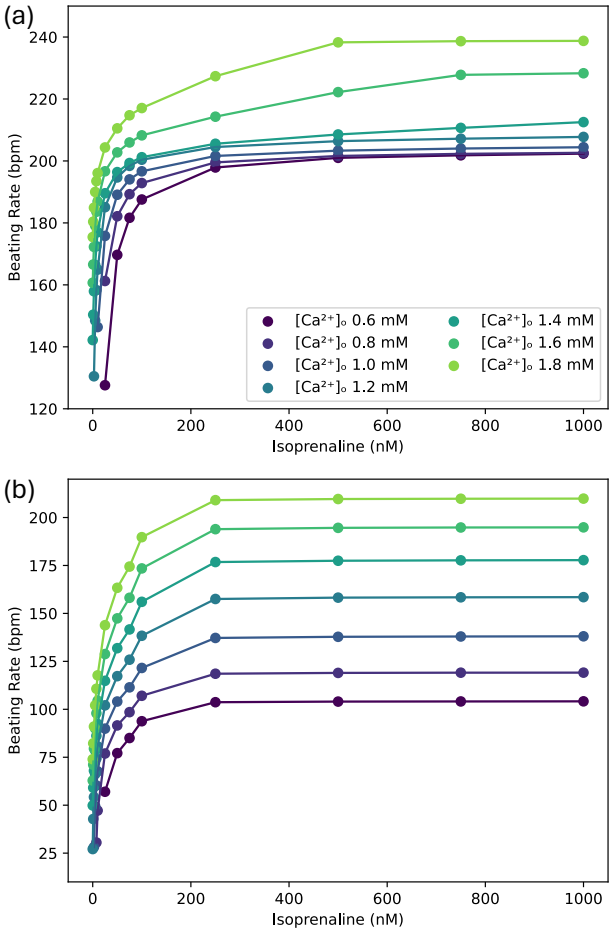

Figure 2: (a) BR dependence for varying [ISO] in the extended Severi et al. rabbit model; (b) in the Fabbri et al. human model. Each line illustrates a different $[Ca^{2+}]_o$.

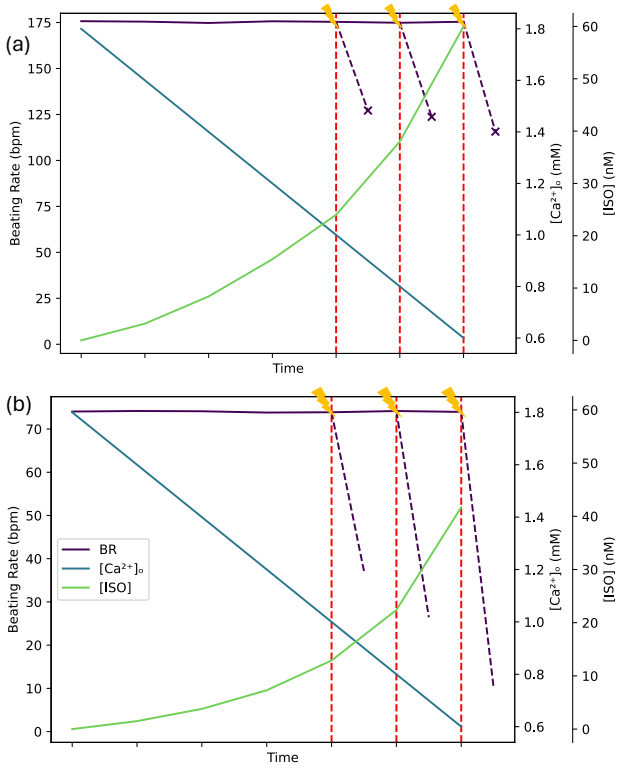

Figure 3: (a) compensatory effect of [ISO] in the extended Severi model; (b) in the extended Fabbri model. Decreased $[Ca^{2+}]_o$ (dark turquoise) was compensated by increased [ISO] (light green) to maintain the basal BR (purple). The red dashed lines indicate three time points at which [ISO] was set to 0.0 nM after simulating the models for 1000 s to reach a steady CL. The purple dashed lines indicate the resulting BRs after a few seconds.

decreased BRs of approximately 115 to 130 bpm before automaticity ceased within a few seconds. In contrast, the extended Fabbri model stabilised after a few seconds with extremely bradycardic BRs of 10 to 35 bpm.

4. Discussion

Both models predicted that bradycardia caused by depletion of $[Ca^{2+}]_o$, as might be occurring in HD patients [3], could be compensated to a certain extent by an increased sympathetic tone. In a recent study, Stary et al. implemented a linear [ISO] dependence in the Fabbri model, which affected the BR almost linearly [11]. Contrary to these findings, the integration of the non-linear β-AR signalling cascade led to an logarithm-like increase of the BR. The sympathetic stimulation affected six different targets, namely: I_{CaL}, I_f, I_{NaK}, I_{Ks}, RyR and SERCA. Three of these targets directly affected the Ca^{2+} cycling between the cell compartments.

As Loewe et al. outlined, the effects of inter-species differences are not negligible [12]. Assessing the most dominant pacemaker current until late DD, I_f and I_{NaCa} were most important in the extended Severi model. In the extended Fabbri model, the impact of I_f is attenuated, which rebalanced the pacemaking control towards I_{CaL}, I_{CaT} and I_{NaCa}. By increasing its conductance and shifting the activation curve, hypocalcemia-induced reduction of Ca^{2+} cycling was directly compensated by the ANS. With less Ca^{2+} available, the [ISO]-mediated effects on the different targets needed to be more pronounced to restore the basal BRs. This led to the exponential-like compensation behaviour. The higher Ca^{2+} and [ISO] sensitivity of the extended Fabbri model can be explained by I_{CaL} being a main pacemaking current.

During the integration process of the β-AR signalling cascade into the SANC models, some assumptions were made to overcome the lack of experimental data. Since,

generation and degradation of intracellular cAMP are influenced by several model parameters, these equations were adjusted to cover the inter-species differences. Besides, the PKA-dependent activation curve shift of I_{CaL} and I_{Ks} was expected to behave similar to the cAMP-mediated activation curve shift of the funny current (I_f). Lastly, the increase in conductance for I_{NaK} and I_{Ks} was assumed to be similar to the PKA-mediated phosphorylation of the L-type Ca^{2+} channel. To ensure a more realistic sympathetic stimulation, channel specific differences in reference to changes in the PKA level should be further investigated.

Verkerk et al. discussed changes in the kinetics of I_{Ks} with respect to β-AR stimulation in human SANCs [13]. Based on the experimental data in HEK-293 cells, the K^+:Na^+ permeability, conductance and reversal potential were adjusted. Including these findings into the extended Fabbri model might impact the BR acceleration. Additionally, the complete integration of the cholinergic receptor stimulation could further enhance the models towards more realistic predictions. This could include simulations with a sudden increase in the parasympathetic tone.

In [3], the Fabbri model was enhanced to capture dynamically changing intracellular K^+ and Na^+ concentrations with a constant basal sympathetic tone. These optimisations resulted in more stability towards lower $[Ca^{2+}]_o$. Further decreases of the Ca^{2+} levels in combination with lower [ISO] might also be of interest to better understand the pathogenesis of hypocalcemia-induced bradycardia.

We assessed automaticity only on single cell level. To capture the excitation initiating the heartbeat *in vivo*, complementing the simulations on single cell level with the surrounding myocardium are necessary [14].

In conclusion, this study strengthens the link between an increased sympathetic tone compensating hypocalcemic bradycardia to a certain extent and an abrupt loss in sympathetic tone (or increase in parasympathetic tone) leading to SCD. This might explain the high prevalence of SCD in CKD patients undergoing HD.

Acknowledgments

This work was supported by DFG-507828355 (CARPediem) and by the European High-Performance Computing Joint Undertaking EuroHPC under grant agreement No 955495 (MICROCARD) co-funded by the Horizon 2020 programme of the European Union (EU), the French National Research Agency ANR, the German Federal Ministry of Education and Research, the Italian ministry of economic development, the Swiss State Secretariat for Education, Research and Innovation, the Austrian Research Promotion Agency FFG, and the Research Council of Norway.

References

[1] Kohajda Z, Loewe A, Tóth N, et al. The cardiac pacemaker story-fundamental role of the Na/Ca exchanger in spontaneous automaticity. Front Pharmacol 1 2020;11:516.

[2] Di Lullo L, Rivera R, Barbera V, et al. Sudden cardiac death and chronic kidney disease: From pathophysiology to treatment strategies. Int J Cardiol 2016-08-15;(217):16–27.

[3] Loewe A, Lutz Y, Nairn D, et al. Hypocalcemia-induced slowing of human sinus node pacemaking. Biophys J 2019-12-17;12(117):2244–2254.

[4] Ishii M, Ikeda T, Takagi M, et al. Elevated plasma catecholamines in hypertensives with primary glomerular diseases. Hypertension 1983-07-01;5(4):545–551.

[5] Converse RL, Jacobsen TN, Toto RD, et al. Sympathetic overactivity in patients with chronic renal failure. N Engl J Med 1992-12-31;27(327):1912–1918.

[6] Severi S, Fantini M, Charawi LA, DiFrancesco D. An updated computational model of rabbit sinoatrial action potential to investigate the mechanisms of heart rate modulation. J Physiol 2012-09-15;18(590):4483–4499.

[7] Fabbri A, Fantini M, Wilders R, Severi S. Computational analysis of the human sinus node action potential: model development and effects of mutations. J Physiol 2017-04-01;7(595):2365–2396.

[8] Cuellar A, Lloyd C, Nielsen P, et al. An overview of CellML 1.1, a biological model description language. Simulation 12 2003;79:740–747.

[9] Behar J, Ganesan A, Zhang J, Yaniv Y. The autonomic nervous system regulates the heart rate through camp-pka dependent and independent coupled-clock pacemaker cell mechanisms. Front in Physiol 2016-09-27;7.

[10] Plank* G, Loewe* A, Neic* A, et al. The openCARP simulation environment for cardiac electrophysiology. Comp Meth Prog Biomed 2021;208:106223.

[11] Stary T, Linder M, Loewe A. Sinoatrial node cell response to isoprenaline stimulation and hypocalcemia. In 2023 Computing in Cardiology (CinC), volume 50. IEEE, 1 2023; .

[12] Loewe A, Lutz Y, Nagy N, et al. Inter-species differences in the response of sinus node cellular pacemaking to changes of extracellular calcium. Annual Int Conference IEEE Eng Med Biol Soc 2019-07;1875–1878.

[13] Verkerk AO, Wilders R. Human sinoatrial node pacemaker activity: Role of the slow component of the delayed rectifier K^+ current, IKs. Int J Mol Sci 2023-04-14;8(24):2764.

[14] Amsaleg A, Sánchez J, Mikut R, Loewe A. Characterization of the pace-and-drive capacity of the human sinoatrial node: A 3d in silico study. Biophys J 11 2022; 121(22):4247–4259.

Address for correspondence:

Institute of Biomedical Engineering
Karlsruhe Institute of Technology (KIT)
Fritz-Haber-Weg 1, 76131 Karlsruhe, Germany
publications@ibt.kit.edu